TECHNICAL DISCLOSURE 01

Graded-Microstructure Bundled Cathode Architecture for Solid Oxide Fuel Cells

Integrated suppression of chromium poisoning, strontium surface segregation, and strontium-zirconate barrier formation

FILER	Coracle Research
PUBLICATION DATE	21 April 2026
PRIMARY VENUE	coracleresearch.com/research/01-bloom-cathode/disclosure.html
PREPRINT DEPOSIT	Zenodo, DOI 10.5281/zenodo.19683758; additional mirror on ChemRxiv pending moderation
LEGAL STATUS	Defensive publication under 35 U.S.C. §102
COMPANION	Research Note 01: Chromium poisoning and the 4.9-year Bloom stack

The subject matter of this disclosure is an integrated cathode-stack architecture for solid oxide fuel cells that addresses, in a single co-fired stack, three compounding cathode-side degradation mechanisms: volatile-chromium poisoning of the active cathode, strontium surface segregation in strontium-doped perovskite cathodes, and strontium-zirconate formation at the cathode-to-electrolyte barrier. The architecture comprises a graded barium-rich perovskite getter sublayer in the cathode air channel, a praseodymium-oxide-infiltrated A-site-deficient $(La,Sr)(Co,Fe)O_{3-\delta}$ cathode, and a low-temperature-densified gadolinium-doped-ceria barrier interposed between the cathode and the yttria-stabilized-zirconia electrolyte.

> *Composition windows, process parameters, alternative embodiments, a worked example, and numbered figures are given below. This document is published as prior art under 35 U.S.C. §102 for defensive purposes as of the publication date above.*

§ 1

Title and Filer

The invention disclosed herein is titled *Graded-Microstructure Bundled Cathode Architecture for Solid Oxide Fuel Cells, providing Integrated Suppression of Chromium Poisoning, Strontium Surface Segregation, and Strontium-Zirconate Barrier Formation*. The filer of record is Coracle Research. The effective publication date is the date stated in the masthead and in the filer block above. A preprint copy of this disclosure is deposited on Zenodo under DOI 10.5281/zenodo.19683758 for examiner-searchable durability, with an additional mirror on ChemRxiv pending moderation, and a PDF paper copy is available for download from the primary venue. A companion narrative research note, referenced above, describes the same subject matter in a more accessible register.

§ 2

Field of the Invention

The invention relates to solid oxide fuel cell (SOFC) technology, and more particularly to cathode-stack architectures for SOFCs operating in the 700 to 900 °C range with strontium-doped perovskite cathodes in the (La,Sr)(Co,Fe)$O_{3-\delta}$ (LSCF) or (La,Sr)MnO_3 (LSM) families, gadolinium-doped ceria ($Ce_{0.9}Gd_{0.1}O_{1.95}$, abbreviated GDC) cathode-to-electrolyte barrier layers, yttria-stabilized zirconia (YSZ) electrolytes, nickel-YSZ cermet anodes, and ferritic stainless-steel interconnects bearing $(Mn,Co)_3O_4$-spinel (MCO) protective coatings. The invention addresses the integrated suppression of cathode-side degradation mechanisms whose simultaneous action determines the service life of commercial planar-SOFC stacks.

§ 3

Background and Prior Art

Three cathode-side degradation mechanisms are known in the published SOFC literature to reduce the useful life of planar stacks operating in the 700 to 900 °C window on humid air oxidant.

Chromium poisoning. Ferritic-stainless-steel interconnects evolve volatile CrO_3(g) and $CrO_2(OH)_2$(g) at SOFC operating temperatures. These species travel with the cathode air stream and react with strontium at the cathode triple-phase boundary to form $SrCrO_4$, an electrochemically inert phase. The mechanism is reviewed in Jiang and Chen (2014), and the thermodynamic and vapor-pressure data underlying it are given in Hilpert et al. (1996), Stanislowski et al. (2007), and Matsuzaki and Yasuda (2000). The dominant commercial mitigation is MCO-spinel coating of the interconnect, which reduces but does not eliminate Cr evolution.

Strontium surface segregation. Strontium-doped perovskite cathodes lose active surface area through thermodynamic segregation of Sr to the cathode surface, where Sr reacts with atmospheric CO_2 and H_2O to form a strontium-rich, electrochemically inert skin. The mechanism is reviewed in Wang et al. (2021), and is documented to proceed in the absence of external Cr exposure.

Strontium-zirconate barrier formation. During co-sintering of cell layers at the 1200 to 1400 °C window, and to a lesser extent during service, Sr diffuses through conventionally sintered GDC barriers and reacts with YSZ at the GDC/YSZ interface to form insulating $SrZrO_3$. The mechanism is reviewed in Mehdi et al. (2023), with Sr-tracer evidence given in Wang et al. (2021).

Individual prior-art interventions against each of the three mechanisms have been published. No publication known to the filer combines all three interventions into a single co-fired cathode-stack architecture processable through a single standard sinter window. The most relevant prior art is enumerated below.

[1] M. Zhou, A. Dogdibegovic, W. Wang, et al., "Long-term stability of SOFC with Pr_2O_x-infiltrated LSCF cathode and Pr-doped ceria barrier," U.S. Department of Energy Office of Fossil Energy report under contract DE-FE0031667 (2022). OSTI 1872368. Discloses infiltration of praseodymium oxide into an LSCF cathode paired with a Pr-doped ceria barrier for long-term Sr-segregation suppression. The closest two-component public precedent. Does not disclose the Ba-rich air-channel getter, does not disclose the low-temperature-densified GDC route, and does not disclose A-site under-stoichiometry in combination with PrO_x infiltration.

[2] B. Niu, W. Zhou, Y. Liu, et al., "Barium-containing cobalt-ferrite cathode with $BaCO_3$ surface coating for SOFC," Advanced Functional Materials 31 (2021). OSTI 1877394. Discloses a Ba-containing cathode composition with a $BaCO_3$ surface coating as a chromium-tolerance measure. Does not disclose the upstream graded-microstructure getter architecture, does not disclose A-site-deficient LSCF with PrO_x infiltration, and does not disclose the low-temperature-densified GDC barrier.

[3] Z. Geisendorfer et al., "Air electrode with strontium getter," U.S. Patent Application Publication 2025/0230562 A1, Bloom Energy Corporation, published July 2025. Discloses a strontium-getter layer in the air electrode using TiO_2, Fe_2O_3, CoO_x, MoO_x, or Nb_2O_5 getter chemistries. Does not disclose the Ba-rich $(Ba,Sr)MnO_3$ or Ba-rich $(Ba,Sr)(Co,Fe)O_3$ getter chemistry, does not disclose grain-size grading within the getter, does not disclose A-site-deficient LSCF with PrO_x infiltration, and does not disclose low-temperature-densified GDC.

[4] A. Pillai et al., "Mn-Co-Cu oxide getter in air flow path," U.S. Patent 10,547,073 B2, Bloom Energy Corporation, granted 2020. Discloses a manganese-cobalt-copper oxide getter in the air flow path for chromium capture. Does not disclose Ba-rich perovskite getter chemistry, does not disclose grain-size grading, and is directed solely to chromium capture (single-mechanism, not integrated).

[5] Bloom Energy Corporation, "Metallic interconnect with manganese-cobalt-oxide spinel coating," U.S. Patent Application Publication 2013/0230792 A1. Discloses the MCO-spinel coating on the cathode-facing side of the ferritic interconnect. Represents the state of the art for commercial Cr-diffusion-barrier coatings against which the present disclosure improves.

[6] E. Mutoro, E. J. Crumlin, M. D. Biegalski, H. M. Christen, Y. Shao-Horn, "Enhanced oxygen reduction activity on surface-decorated perovskite thin films for solid oxide fuel cells," Energy & Environmental Science 4 (2011) 3689, DOI 10.1039/C1EE01245B. Foundational study disclosing PrO_x and related rare-earth-oxide surface decoration of $La_{0.8}Sr_{0.2}CoO_{3-\delta}$ as a means of enhancing cathode oxygen-reduction kinetics and suppressing Sr surface enrichment. Does not disclose A-site-deficient bulk LSCF in combination with PrO_x infiltration, does not disclose the upstream Ba-rich getter sublayer, and does not disclose low-temperature-densified GDC.

[7] X. Chen, N. Ai, K. O'Donnell, S. P. Jiang, "BaO-infiltrated LSCF cathode," Phys. Chem. Chem. Phys. 17 (2015), DOI 10.1039/C4CP04172K. Discloses wet infiltration of barium oxide into an LSCF cathode as a chromium-tolerance measure. Places the Ba species inside the cathode body rather than in an upstream air-channel sublayer, does not disclose grain-size grading, and does not disclose the companion A-site-deficient cathode and low-temperature-densified GDC components.

[8] C. Balice et al., "Flash-sintered gadolinium-doped ceria thin barriers for SOFCs," Journal of the American Ceramic Society 108 (2025), DOI 10.1111/jace.70033. Discloses flash-sintered GDC barriers with applied electric field during densification. Directed to the barrier alone; does not disclose the upstream getter or the infiltrated cathode.

[9] M. Mehdi et al., "Durability of SOFC cathodes: a review," Renewable and Sustainable Energy Reviews (2023). Comprehensive review establishing the prior-art landscape for cathode-side degradation.

[10] W. Wang, C. Su, Y. Wu, R. Ran, Z. Shao, "Progress in solid oxide fuel cells with strontium-doped perovskite cathodes: strontium segregation and its suppression," Electrochemical Energy Reviews 4 (2021). Review of Sr-segregation mechanisms and suppression approaches.

[11] S. P. Jiang, X. Chen, "Chromium deposition and poisoning of cathodes of solid oxide fuel cells: a review," International Journal of Hydrogen Energy 39 (2014) 505.

[12] K. Hilpert, D. Das, M. Miller, D. H. Peck, R. Weiß, "Chromium vapor species over solid oxide fuel cell interconnect materials," J. Electrochem. Soc. 143 (1996) 3642.

[13] M. Stanislowski et al., "Chromium vaporization from high-temperature alloys," J. Electrochem. Soc. 154 (2007) A295.

[14] Y. Matsuzaki, I. Yasuda, "Electrochemical properties of a SOFC cathode in contact with a chromium-containing alloy separator," Solid State Ionics 132 (2000) 271.

[15] Standard thermochemical compilations for ΔG_f values of $BaCrO_4$, $SrCrO_4$, $CaCrO_4$, and $MgCrO_4$ used in the thermodynamic ladder of Figure 3, including NIST-JANAF Thermochemical Tables, 4th Ed., and I. Barin, *Thermochemical Data of Pure Substances*, 3rd Ed., Wiley-VCH (1995 / reprint 2004). Anchor values for $BaCrO_4$ and $SrCrO_4$ vary across compilations ($BaCrO_4$ reported from approximately −1345 to −1380 kJ/mol; $SrCrO_4$ from approximately −1281 to −1306 kJ/mol); the approximately 60 to 80 kJ/mol Ba-to-Sr gap that underlies the disclosed thermodynamic redirection is consistent across all tabulations.

An additional body of work on wet-infiltration enhancement of SOFC cathodes with praseodymium, cerium, and related rare-earth oxides has been published across the 2015 to 2024 window by groups at Northwestern University (Barnett and colleagues), Forschungszentrum Jülich, Curtin University (Jiang and colleagues), Georgia Institute of Technology (Liu and colleagues), and the U.S. Department of Energy national-laboratory SOFC program, in addition to the specific entries cited above. The present disclosure extends that body of work by combining PrO_x infiltration with A-site-deficient bulk LSCF, with the upstream graded Ba-rich getter sublayer, and with the low-temperature-densified GDC barrier as an integrated cathode-stack architecture processable through a single cell sinter and a single interconnect-subassembly sinter.

The distinction of the present disclosure over the cited art is the integration of all three interventions on a single cathode-stack assembly processable through one standard co-fire window. The individual components draw on and extend public work. The integrated architecture, and the specific compositional and processing windows that enable integration without introducing firing steps above the conventional SOFC peak-sinter temperature, are not disclosed in the cited art.

§ 4

Summary of the Invention

The present invention provides an integrated solid-oxide-fuel-cell cathode-stack architecture comprising, in ordered arrangement from the cathode air channel toward the electrolyte:

Component A. Graded Ba-rich perovskite getter sublayer

A porous perovskite sublayer of total thickness 2 to 5 μm, positioned in the cathode air channel immediately upstream of the active cathode, with a continuous grain-size gradient from 100 to 300 nm on the air-channel-facing side to 500 nm to 1 μm on the cathode-interface-facing side, and a Ba-rich perovskite composition selected from the (Ba,Sr)MnO_3 family at Ba/Sr ≥ 2:1 molar or the Ba-rich (Ba,Sr)(Co,Fe)$O_{3-\delta}$ family, selected to satisfy thermal-expansion-coefficient compatibility with the adjacent LSCF cathode and GDC barrier.

Component B. PrO_x-infiltrated A-site-deficient LSCF cathode

A (La,Sr)(Co,Fe)$O_{3-\delta}$ cathode of A-site stoichiometry (La+Sr)/(Co+Fe) in the range 0.95 to 0.98, infiltrated after fabrication with 2 to 5 weight percent praseodymium oxide deposited from a 0.5 to 1.0 M aqueous $Pr(NO_3)_3$ solution and thermally decomposed at 500 to 600 °C, yielding dispersed PrO_x islands of 10 to 50 nm in diameter at below 10 percent external-surface coverage.

Component C. Low-temperature-densified GDC barrier

A gadolinium-doped-ceria barrier of composition $Ce_{0.9}Gd_{0.1}O_{1.95}$, densified to greater than 97 percent theoretical density at a peak processing temperature of 1100 °C or below, by a process selected from spark-plasma sintering (900 to 1100 °C, 50 to 100 MPa uniaxial, 3 to 5 minute dwell), flash sintering (50 to 200 V/cm applied field with sample temperature 700 to 900 °C and current limit 5 to 15 mA/mm^2), or atomic-layer deposition (200 to 300 °C substrate temperature, 100 to 500 nm deposited thickness, from cerium and gadolinium β-diketonate precursors with ozone co-reactant).

The three components, in combination, are processable through a single standard co-fire window for the cell in the 1200 to 1400 °C range, with post-sinter wet infiltration of Component B and pre-stack densification of Component C. The combination suppresses all three named cathode-side degradation mechanisms concurrently, by three independent and compatible physical mechanisms: thermodynamic Cr capture on a Ba-rich surface upstream of the active cathode (Component A), A-site chemical-potential elevation and surface capping against Sr egress (Component B), and closure of the Sr-diffusion pathway from the cathode to the YSZ electrolyte during both manufacture and operation (Component C).

Quantitative performance target: baseline planar-SOFC cells on LSCF-GDC-YSZ chemistry in accelerated-aging tests at 800 °C with 3 percent H_2O in cathode air and a simulated Cr_2O_3 vapor source exhibit area-specific resistance (ASR) growth in the range 3× to 5× over 2000 hours. Cells built according to the present disclosure are predicted to exhibit less than 2× ASR growth over the same interval. The improvement is multiplicative at the stack level and is expected to close the majority of

the cathode-side contribution to observed lifetime gaps in deployed planar-SOFC stacks. Residual stack degradation channels, including anode Ni coarsening, interconnect scale growth, and glass-seal aging, are outside the scope of the present disclosure and are addressable by separate interventions.

§ 5

Detailed Description of the Preferred Embodiment

The preferred embodiment is described below in four subsections. Subsection 5.1 specifies the graded Ba-rich getter sublayer (Component A). Subsection 5.2 specifies the PrO_x-infiltrated A-site-deficient LSCF cathode (Component B). Subsection 5.3 specifies the low-temperature-densified GDC barrier (Component C). Subsection 5.4 specifies the integration architecture, layer-stack order, and co-fire schedule. Numbered reference elements consistent with the figures in Section 10 are used throughout the description for unambiguous mapping between text and drawings.

REFERENCE NUMERAL KEY (USED THROUGHOUT §5 AND FIGURES)

10	First ferritic stainless-steel interconnect (cathode-air side)
20	$(Mn,Co)_3O_4$ spinel protective coating on the cathode-facing face of interconnect 10
30	Cathode air channel
40	Graded Ba-rich perovskite getter sublayer (Component A)
40a	Fine-grain region of sublayer 40, facing air channel 30
40b	Coarse-grain region of sublayer 40, facing cathode 50
50	PrO_x-infiltrated A-site-deficient LSCF cathode (Component B)
50a	Bulk LSCF matrix of cathode 50
50b	PrO_x surface islands on cathode 50
60	Low-temperature-densified GDC barrier (Component C)
70	YSZ electrolyte
80	Ni-YSZ cermet anode
90	Fuel channel
100	Second ferritic stainless-steel interconnect (fuel side)

§ 5.1 Graded Ba-rich Perovskite Getter Sublayer (40)

The getter sublayer (40) is a porous Ba-rich perovskite layer deposited on the cathode-facing face of the interconnect-side gas channel assembly and positioned in the cathode air channel (30) immediately upstream of the active cathode (50), such that every gas streamline carrying volatile chromium species from interconnect 10 must pass through sublayer 40 before contacting cathode 50. The layer suppresses chromium poisoning of cathode 50 by the reaction

$$SrO(s,\ in\ LSCF) + CrO_3(g) \rightarrow SrCrO_4(s)$$

through thermodynamic redirection to the reaction

$$BaO(s,\ in\ sublayer\ 40) + CrO_3(g) \rightarrow BaCrO_4(s)$$

which carries a Gibbs free energy of formation on the order of 60 to 80 kJ/mol more negative than the corresponding strontium reaction across the SOFC operating-temperature range (700 to 900 °C). Representative values of $\Delta G_f(BaCrO_4)$ near −1380 kJ/mol and $\Delta G_f(SrCrO_4)$ near −1306 kJ/mol are taken from standard thermochemical compilations. Anchor values vary by compilation ($BaCrO_4$ in the range −1345 to −1380 kJ/mol; $SrCrO_4$ in the range −1281 to −1306 kJ/mol across published tabulations); the Ba-to-Sr gap underlying the disclosed thermodynamic redirection is consistent at approximately 60 to 80 kJ/mol across all tabulations. Values are plotted with comparison compounds in Figure 3.

Composition

The getter composition of sublayer 40 is selected from a Ba-rich perovskite family. Preferred compositions are (i) (Ba,Sr)MnO_3 with a Ba:Sr molar ratio of 2:1 or greater, with a preferred nominal composition of $Ba_{0.7}Sr_{0.3}MnO_3$, and (ii) Ba-rich (Ba,Sr)(Co,Fe)$O_{3-\delta}$ with a Ba:Sr molar ratio of 2:1 or greater and a Co:Fe ratio in the range 0.2:0.8 to 0.5:0.5, with a preferred nominal composition of $Ba_{0.8}Sr_{0.2}Co_{0.2}Fe_{0.8}O_{3-\delta}$. The specific composition is selected within the above family to satisfy thermal-expansion-coefficient compatibility with adjacent cathode 50 and barrier 60, targeting a coefficient of thermal expansion in the range 10×10^{-6} to 13×10^{-6} K^{-1} averaged over 25 to 800 °C.

Total thickness

The total thickness of sublayer 40 is in the range 2 to 5 μm measured normal to the layer plane, with 3 μm as the preferred value. Thickness is sized so that the integrated BaO mass per unit cell area exceeds the cumulative chromium flux per unit cell area expected across the intended service life of the stack by a factor of 2 or more.

Grain-size gradient

The grain-size distribution of sublayer 40 varies continuously along the through-thickness coordinate. At the air-channel-facing surface of sublayer 40 (defined as region 40a), the mean grain diameter is in the range 100 to 300 nm, with a preferred value near 150 nm. At the cathode-interface-facing surface of sublayer 40 (defined as region 40b), the mean grain diameter is in the range 500 nm to 1 μm, with a preferred value near 800 nm. The gradient is monotonic from 40a to 40b and may be continuous or stepped in two or more sub-zones. The grain gradient is shown in Figure 2.

Porosity

The through-thickness open porosity of sublayer 40 is in the range 25 to 45 volume percent to enable unimpeded gas transport while maintaining structural integrity. Fine-grain region 40a has preferred open porosity near 30 percent. Coarse-grain region 40b has preferred open porosity near 40 percent.

Green-tape formulation

The green tape for sublayer 40 comprises a bimodal particle-size distribution, with fine fraction of nominal mean diameter 50 to 100 nm and coarse fraction of nominal mean diameter 300 to 500 nm, in a fine:coarse volume ratio selected in the range 3:1 to 1:1 to produce the post-sinter grain gradient after controlled firing. The tape uses a standard poly(vinyl butyral) / dibutyl phthalate binder-plasticizer system compatible with the cell's existing tape-cast flow, with a solids loading of 55 to 65 volume percent.

Deposition method

The preferred deposition method for sublayer 40 is tape casting onto the assembled cathode-side green stack, with the fine-fraction-enriched tape face oriented toward the prospective air channel. Alternative deposition methods include screen printing with sequential fine-then-coarse paste layers, slurry spraying with composition grading, and freeze-cast lamellar structures oriented normal to the gas-flow direction.

Sintering

Sublayer 40 is sintered as part of the interconnect-side subassembly per the fabrication sequence of §5.4, with peak temperature in the range 1250 to 1350 °C for the preferred compositions above. Dwell time at peak is 2 to 5 hours, with heating rate 3 to 5 °C/min and cooling rate 3 to 5 °C/min. The Ba-rich perovskite compositions above begin densifying at 1100 to 1150 °C and reach the target microstructure within the stated window. Compositions that densify only above 1500 °C are explicitly excluded. Alternative integration routes in which sublayer 40 is sintered together with other cell components are within the scope of §6.6.

§ 5.2 PrO_x-Infiltrated A-site-Deficient LSCF Cathode (50)

The cathode (50) is a mixed ionic-electronic conducting perovskite that performs oxygen reduction at the cathode side of the cell. The present disclosure modifies cathode 50 against strontium surface segregation by two compositional means acting in combination: under-stoichiometry of the A-site sublattice relative to the B-site sublattice in the bulk LSCF matrix 50a, and deposition of praseodymium-oxide surface islands 50b by post-fabrication wet infiltration.

Bulk LSCF composition

The bulk cathode matrix 50a is a strontium-lanthanum-cobalt-ferrite perovskite of general formula $(La,Sr)_{1-x}(Co,Fe)O_{3-\delta}$ where the A-site deficit x is in the range 0.02 to 0.05, corresponding to an A-site-to-B-site stoichiometric ratio (La+Sr)/(Co+Fe) in the range 0.95 to 0.98. The preferred nominal composition is $La_{0.58}Sr_{0.4}Co_{0.2}Fe_{0.8}O_{3-\delta}$, giving (La+Sr)/(Co+Fe) = 0.98. The La:Sr ratio within the A-site sublattice is maintained at the conventional value of approximately 3:2 (La/Sr near 1.5). The Co:Fe ratio within the B-site sublattice is 0.2:0.8, matching the composition of commercial LSCF cathode powder.

Mechanism of Sr-segregation suppression (compositional)

The A-site deficit raises the chemical potential of A-site cations in the bulk perovskite lattice and thereby reduces the thermodynamic driving force for Sr egress to the cathode free surface. The bulk electrical conductivity penalty associated with the stated deficit range is below 5 percent relative to stoichiometric LSCF and is accepted as a favorable trade against Sr-segregation kinetics over service-relevant timescales.

Cathode microstructure

Cathode 50 is a porous layer of thickness 15 to 30 μm (preferred 20 μm), with open porosity 25 to 40 volume percent and mean grain size in the range 250 to 500 nm. The cathode is produced by standard screen-printing or tape-casting of LSCF powder of the A-site-deficient composition specified above, followed by co-sintering in the 1050 to 1150 °C window to produce a well-bonded, sufficiently porous layer that retains the compositional A-site deficit on firing.

PrO_x infiltration precursor and solution

The PrO_x surface islands 50b are deposited onto cathode 50 by wet infiltration after sintering of cathode 50 but before final cell-stack assembly. The infiltrating solution is an aqueous solution of praseodymium nitrate hexahydrate, $Pr(NO_3)_3{\cdot}6H_2O$, at concentration 0.5 to 1.0 M, with 0.75 M as the preferred value. A surfactant such as Triton X-100 at 0.1 to 0.5 weight percent may be added to improve wetting of the porous LSCF microstructure.

Infiltration protocol

The porous sintered cathode 50 is infiltrated by a combination of vacuum infiltration (5 to 60 seconds under 10^{-1} to 10^{-2} atm vacuum) followed by ambient release, repeated for 3 to 5 cycles to reach the target PrO_x loading. Between cycles, the cell is dried at 80 to 120 °C. Total PrO_x loading after decomposition is 2 to 5 weight percent of the finished cathode, with 3 weight percent as the preferred value.

Thermal decomposition

Following the final infiltration cycle, the cell is fired at 500 to 600 °C (preferred 550 °C) in ambient air for 1 to 2 hours with heating rate 2 to 3 °C/min. The decomposition step converts deposited $Pr(NO_3)_3$ to a PrO_x phase of nonstoichiometric oxidation state (predominantly Pr_6O_{11} with minor PrO_2), dispersed as surface islands on the LSCF grain surfaces.

PrO_x island morphology

The decomposed PrO_x forms surface islands 50b of mean diameter 10 to 50 nm (preferred 20 to 30 nm) covering less than 10 percent of the LSCF external surface area (preferred 5 to 8 percent). Islands are distributed on both the gas-channel-facing surface of cathode 50 and the internal surfaces of the porous cathode network reached by the infiltrating solution.

Mechanism of Sr-segregation suppression (surface)

The PrO_x islands are electrochemically active for oxygen reduction at cathode operating temperature and provide alternative oxygen-incorporation sites that relieve local driving force for Sr accumulation at the LSCF surface. The islands additionally present a geometric barrier to continued Sr egress on the regions of the surface they cover. The surface and bulk mechanisms compose multiplicatively: A-site deficiency reduces the driving force, and PrO_x caps the remaining susceptible surface area.

§ 5.3 Low-Temperature-Densified GDC Barrier (60)

The barrier (60) is a thin gadolinium-doped-ceria interlayer between cathode 50 and electrolyte 70 that prevents the Sr-Zr reaction forming insulating $SrZrO_3$ at the cathode/electrolyte interface. The present disclosure departs from conventional co-sintered GDC barriers by densifying barrier 60 at a process temperature in which bulk Sr diffusion is thermodynamically suppressed.

Composition

The barrier composition is $Ce_{1-x}Gd_xO_{2-x/2}$ with x in the range 0.10 to 0.20. The preferred composition is $Ce_{0.9}Gd_{0.1}O_{1.95}$ (GDC10) for maximum ionic conductivity at intermediate SOFC temperatures. Alternative dopants in the rare-earth-doped ceria family, including samarium-doped ceria (SDC) and yttrium-doped ceria (YDC), are within the scope of the disclosure.

Target density and thickness

Barrier 60 is densified to greater than 97 percent of theoretical density, with 98 to 99 percent as the preferred value. Total layer thickness is in the range 100 nm to 5 µm depending on the densification process, with 1 to 3 µm preferred for the spark-plasma and flash routes and 100 to 500 nm preferred for the atomic-layer deposition route.

Three alternative densification processes are disclosed. Each reaches the target density at a peak processing temperature at which bulk Sr diffusion through barrier 60 is suppressed by three orders of magnitude or more relative to conventional 1400 °C co-sintering.

Route 1. Spark-plasma sintering (SPS)

GDC powder of mean particle diameter 50 to 200 nm is loaded into a graphite die of appropriate geometry for the cell dimensions and sintered under a uniaxial pressure of 50 to 100 MPa (preferred 80 MPa). The applied DC pulsed current heats the sample to a peak temperature of 900 to 1100 °C (preferred 1000 °C), with a heating rate of 50 to 200 °C/min and a dwell of 3 to 5 minutes at peak. Ambient is low vacuum (10 Pa) or flowing argon. The resulting barrier has a density of 98 to 99 percent theoretical and a grain size of 200 to 500 nm.

Route 2. Flash sintering

A pressed-and-bisque-fired GDC tape or disc is placed between conductive electrodes with an applied AC or DC electric field of 50 to 200 V/cm (preferred 100 V/cm) and heated in a conventional furnace at 10 to 20 °C/min. At a critical furnace temperature of 700 to 900 °C (dependent on field strength and composition), a runaway flash event occurs in which the sample temperature spikes by 200 to 400 °C and densification completes in 5 to 30 seconds. The flash event is limited by a power cap corresponding to a current density of 5 to 15 mA/mm^2 (preferred 10 mA/mm^2) to prevent local melting and grain-boundary darkening. The resulting barrier has a density of 97 to 98 percent theoretical and a grain size of 300 to 800 nm.

Route 3. Atomic-layer deposition (ALD)

Barrier 60 is deposited onto the pre-sintered YSZ electrolyte (70) by thermal ALD at a substrate temperature of 200 to 300 °C (preferred 250 °C). Precursors are cerium(III) tris(2,2,6,6-tetramethyl-3,5-heptanedionate) (abbreviated $Ce(tmhd)_3$) and gadolinium(III) tris(2,2,6,6-tetramethyl-3,5-heptanedionate) ($Gd(tmhd)_3$), introduced alternately with ozone (O_3) as the oxygen co-reactant. Cerium:gadolinium pulse ratio is tuned to produce the target 9:1 cation ratio in the deposited film. Deposition rate is approximately 0.5 to 1 Å per supercycle. Film thickness is 100 to 500 nm (preferred 200 nm). A subsequent low-temperature crystallization anneal at 600 to 800 °C converts the as-deposited amorphous film to the fluorite phase without exposing the stack to the Sr-diffusion window.

All three routes keep peak processing temperature at or below 1100 °C, which is 100 to 300 °C below the conventional 1200 to 1400 °C co-sinter window at which Sr free-diffuses through a conventionally sintered GDC barrier. At these reduced temperatures, Sr bulk diffusivity in GDC is reduced by three to four orders of magnitude relative to conventional co-sintering, and the dense microstructure (exceeding 97 percent theoretical) closes the fast grain-boundary diffusion path that dominates residual Sr transport in partially densified GDC. Both the manufacturing-stage $SrZrO_3$ layer and the in-service Sr flux are suppressed.

§ 5.4 Integration Architecture and Co-Fire Schedule

The layer-stack order, proceeding from the cathode-air-side interconnect (10) toward the fuel-side interconnect (100), is: interconnect 10; MCO spinel coating 20 on the cathode-facing surface of interconnect 10; air channel 30; graded Ba-rich perovskite getter sublayer 40 (with fine-grain region 40a facing air channel 30 and coarse-grain region 40b facing cathode 50); PrO_x-infiltrated A-site-deficient LSCF cathode 50 (with PrO_x surface islands 50b on bulk LSCF matrix 50a); low-temperature-densified GDC barrier 60; YSZ electrolyte 70; Ni-YSZ cermet anode 80; fuel channel 90; second interconnect 100. A full cross-section of the repeat unit is given in Figure 1.

Fabrication sequence

The preferred fabrication sequence, in order, is: (i) fabrication of the anode-supported half-cell by tape-casting of anode 80 and YSZ electrolyte 70 followed by co-sintering at 1350 to 1400 °C for 2 to 4 hours; (ii) deposition of the low-temperature-densified GDC barrier 60 onto the electrolyte face of the half-cell by one of the three routes described in § 5.3; (iii) screen-printing or tape-casting of the A-site-deficient LSCF cathode 50 onto barrier 60, followed by cathode sintering at 1050 to 1150 °C for 2 to 3 hours; (iv) wet infiltration of cathode 50 with the $Pr(NO_3)_3$ precursor solution and thermal decomposition per § 5.2; (v) separate processing of the interconnect-side subassembly, comprising the MCO-coated interconnect 10 with graded getter sublayer 40 deposited by tape casting, green-laminated with fine-face toward the prospective air channel and sintered at 1200 to 1350 °C for 2 to 4 hours; (vi) final stack assembly by placement of the interconnect subassembly onto the PrO_x-infiltrated cell with appropriate glass-seal materials around the gas-channel perimeter, followed by seal-bond firing at 850 to 900 °C.

Compatibility with the conventional co-fire window

The sequence above uses a single cell co-sinter in the 1350 to 1400 °C window for the half-cell, and a single interconnect-subassembly sinter in the 1200 to 1350 °C window for the getter. Cathode sintering and PrO_x decomposition occur at substantially lower temperatures (1050 to 1150 °C and 500 to 600 °C respectively) at which bulk Sr diffusion is suppressed. The GDC densification route is chosen to match the chosen cell fabrication flow: SPS is compatible with a pre-assembled half-cell, flash sintering is compatible with a standalone barrier tape laminated prior to cathode deposition, and ALD is compatible with any geometry of pre-sintered electrolyte. The integration architecture adds no firing step above the conventional SOFC peak-sinter temperature: the additional process steps (low-temperature GDC densification; interconnect-subassembly sinter with sublayer 40; and PrO_x decomposition bake) operate at peak temperatures at or below the conventional SOFC sinter window, preserving stack-level thermal-expansion compatibility and seal-bond thermal history.

Thermal-expansion-coefficient matching

All cathode-side materials (sublayer 40, cathode 50, barrier 60) are selected within the 10×10^{-6} to 13×10^{-6} K^{-1} thermal-expansion-coefficient window, referenced to the 25 to 800 °C operating window. A-site-deficient LSCF with the preferred composition has a measured TEC of approximately 15×10^{-6} K^{-1} and is managed by graded porosity at the cathode/barrier interface and by control of the cathode thickness below 30 μm to constrain absolute in-plane strain. The Ba-rich $(Ba,Sr)MnO_3$ getter has a TEC of approximately 11×10^{-6} K^{-1} and is compatible with the cathode side without further modification.

Operating envelope

The integrated cathode-stack architecture is specified for planar SOFCs operating in the range 700 to 900 °C with humid air (0 to 5 volume percent H_2O) on the cathode side, with an open-circuit voltage of approximately 1.1 V per cell and a current-density operating envelope of 0.3 to 0.8 A/cm^2. The architecture is not specified for operation above 900 °C, where the Ba-rich getter perovskite undergoes accelerated sintering and loses porosity, or below 650 °C, where LSCF oxygen-reduction kinetics become limiting.

§ 6

Alternative Embodiments

Alternative embodiments of each of the three disclosed components, and alternative architectures combining them, are enumerated below. The enumeration is included to foreclose design-around efforts that would substitute a nominally different means for one or more disclosed components while preserving the integrated architecture.

§ 6.1 Alternative getter compositions for sublayer (40)

Without limitation to the $(Ba,Sr)MnO_3$ and Ba-rich $(Ba,Sr)(Co,Fe)O_{3-\delta}$ compositions of §5.1, the following Ba-rich or Ba-bearing getter chemistries are disclosed as covered variants:

- $(Ba,Ca)MnO_3$ family with Ba:Ca molar ratios in the range 1:1 to 4:1.
- Pure $BaMnO_3$ in hexagonal or perovskite polytype, thermally treated as appropriate to the target polymorph.
- $BaCo_{0.5}Mn_{0.5}O_{3-\delta}$ and related Ba-rich Co-Mn perovskites.
- $BaFe_{12}O_{19}$ hexaferrite as a non-perovskite Ba-rich getter.
- Ba-rich La-Mn perovskites of general form $(La,Ba)MnO_3$ with Ba mole fraction ≥ 0.3.
- Ruddlesden-Popper K_2NiF_4-structure oxides in the Ba-Mn and Ba-Fe families, including Ba_2MnO_4 and analogous compositions.
- Solid-solution Ba-perovskites with Bi, Zr, or Nb B-site substitutions for thermal-expansion-coefficient tuning.
- BaO- or $BaCO_3$-coated LSCF or LSM cathode surfaces as a less-preferred variant in which the Ba species is located within the cathode body rather than in an upstream sublayer.

§ 6.2 Alternative cathode Sr-suppression means

Without limitation to the A-site-deficient PrO_x-infiltrated LSCF cathode of §5.2, the following cathode Sr-segregation-suppression means are disclosed:

- CeO_x infiltration at 2 to 5 weight percent in place of, or in combination with, PrO_x, from $Ce(NO_3)_3{\cdot}6H_2O$ aqueous precursor.
- MnO_x infiltration at 1 to 3 weight percent from $Mn(NO_3)_2{\cdot}xH_2O$ precursor.
- Cobalt-spinel infiltration with Co_3O_4 or Co-containing spinel compositions at 2 to 5 weight percent.
- Tighter A-site under-stoichiometry in the range 0.90 to 0.95, accompanied by an appropriate surface-infiltration cap.
- Co-infiltration of PrO_x with Ce or Mn, applied sequentially or from a mixed-metal nitrate solution.
- Substitution of the LSCF matrix by barium-strontium-cobalt-ferrite (BSCF, $Ba_{0.5}Sr_{0.5}Co_{0.8}Fe_{0.2}O_{3-\delta}$) or lanthanum-nickelate ($La_2NiO_{4+\delta}$) cathode chemistries, with A-site deficit and PrO_x infiltration applied analogously.

§ 6.3 Alternative GDC-barrier densification routes

Without limitation to the three routes of §5.3, the following low-temperature densification routes for the GDC barrier are disclosed:

- Microwave-assisted sintering at 900 to 1100 °C peak temperature under applied microwave field at 2.45 GHz or higher frequency.
- Cold sintering at 200 to 400 °C with an aqueous transient-liquid-phase sintering aid selected from $Ce(OH)_4$ suspension, ammonium carbonate solution, or $Ce(NO_3)_3$ flux.
- Hybrid SPS-flash (pulsed-electric-current sintering) configurations combining uniaxial pressure and applied DC field in one densification step.
- Reactive sputtering or RF sputtering of GDC at ambient substrate temperature followed by low-temperature crystallization anneal below 800 °C.
- Pulsed-laser deposition (PLD) of GDC at substrate temperature below 500 °C with post-deposition anneal.
- Electrochemical densification through applied voltage across the deposited GDC film during low-temperature anneal.

- Composite or graded barriers using alternative Sr-immobile buffer species (Pr-doped ceria, Sm-doped ceria, Y-doped ceria) as bilayer or continuously graded structures interposed between cathode 50 and electrolyte 70.

§ 6.4 Alternative grain-grading profiles for sublayer (40)

Without limitation to the continuous grain-size gradient of §5.1 from 100-300 nm at region 40a to 500-1000 nm at region 40b, the following grain-grading profiles are disclosed:

- Stepped gradient with two or more discrete grain-size zones separated by sharp or diffuse boundaries.
- Exponential or power-law gradient with steeper grain-size change concentrated near the air-channel interface.
- Inverted gradient (coarse at air-channel face, fine at cathode-interface face) for applications in which grain-boundary diffusion downstream of the capture zone is rate-limiting.
- Trilayer gradient with an ultra-fine top layer (< 100 nm grain size) for kinetic capture, a mid-range middle layer for capacity, and a coarse bottom layer for low-impedance gas transport.
- Porosity grading applied in combination with, or in substitution for, grain-size grading.

§ 6.5 Reactive-element additions to sublayer (40)

Without limitation to the baseline compositions of §5.1, the addition of rare-earth or reactive-element (RE) dopants to sublayer 40 in the range 0.5 to 10 mole percent (cation basis) is disclosed as an alternative embodiment providing grain-boundary stabilization against in-service coarsening of sublayer 40, thermal-expansion-coefficient tuning, and oxygen-vacancy-chemistry modification:

- Yttrium (Y) at 1 to 5 mole percent on A-site or B-site positions.
- Lanthanum (La) at 1 to 10 mole percent as an A-site partial substitute.
- Zirconium (Zr) at 0.5 to 3 mole percent on the B-site for TEC tuning.
- Cerium (Ce) at 1 to 3 mole percent on the B-site.
- Combined Y+Zr, Y+La, or Y+Ce co-doping at 1 to 5 mole percent total.

§ 6.6 Alternative architectures integrating the three disclosed components

Beyond the ordered-layer-stack architecture of §5.4, the following alternative integrated architectures combining the three disclosed components are covered:

- Cathode-integrated getter, in which a Ba-rich getter phase is dispersed throughout the cathode bulk 50a as a second-phase inclusion, in addition to its concentration in sublayer 40.
- Multi-sublayer getter, in which two or more distinct Ba-rich compositions are stacked at different through-thickness positions within air channel 30.
- Interconnect-integrated getter, in which sublayer 40 is deposited directly onto the MCO coating 20 of interconnect 10 as a combined coating rather than as a free-standing layer.
- Tubular-SOFC adaptation, in which the ordered-layer-stack architecture of §5.4 is wrapped concentrically around a tubular cathode-supported or anode-supported geometry.
- Reversible SOFC/SOEC adaptation, in which the integrated cathode architecture is applied to the oxygen-electrode side of a reversible solid-oxide cell operated alternately in fuel-cell and electrolysis modes, with composition windows selected for compatibility with higher current densities and more extreme polarization.

§ 7

Worked Example

The worked example below presents one specific embodiment of the integrated cathode-stack architecture at point values within the disclosed ranges of §5. The example is illustrative and does not limit the scope of the disclosure. The point values in this §7 derive from published SOFC-materials literature and represent a self-consistent starter configuration suitable for reduction to practice by a POSITA.

Cell geometry

10 cm × 10 cm planar cell, anode-supported geometry.

Anode support (80)

Thickness 200 µm; composition 50:50 volume ratio Ni:YSZ (8YSZ); open porosity 30 volume percent after reduction; tape-cast and laminated.

YSZ electrolyte (70)

Thickness 10 µm; composition $Zr_{0.92}Y_{0.08}O_{1.96}$ (8YSZ); co-sintered with anode support at 1350 °C for 3 hours.

GDC barrier (60)

Thickness 3 µm; composition $Ce_{0.9}Gd_{0.1}O_{1.95}$; densification route: spark-plasma sintering at 1000 °C peak temperature, 80 MPa uniaxial pressure, 4-minute dwell at peak, 100 °C/min heating and cooling, argon ambient; resulting density 98.5 percent of theoretical; resulting mean grain size 400 nm.

LSCF cathode (50), PrO_x-infiltrated

Thickness 20 µm; bulk composition $La_{0.58}Sr_{0.4}Co_{0.2}Fe_{0.8}O_{3-\delta}$ (A-site-to-B-site ratio 0.98); cathode sintering at 1100 °C for 2 hours; PrO_x loading 3 weight percent of finished cathode; infiltration precursor 0.75 M aqueous $Pr(NO_3)_3{\cdot}6H_2O$; 4 vacuum-infiltration cycles at 10^{-2} atm each followed by ambient release; thermal decomposition at 550 °C for 1.5 hours in ambient air; resulting PrO_x island diameter 20 to 30 nm mean; resulting external-surface PrO_x coverage 6 to 8 percent.

Graded Ba-rich getter sublayer (40)

Total thickness 3 µm; composition $Ba_{0.7}Sr_{0.3}MnO_3$; fine-grain region 40a of 1.5 µm thickness with mean grain diameter 150 nm; coarse-grain region 40b of 1.5 µm thickness with mean grain diameter 800 nm; deposition by bimodal-particle-size-distribution tape casting onto the interconnect-side subassembly; sintering at 1300 °C for 3 hours (3 °C/min heating rate, 3 °C/min cooling rate).

MCO coating (20)

Thickness 15 µm; composition $(Mn_{1.5}Co_{1.5})O_4$ spinel; deposition by atmospheric plasma spray with post-deposition densification bake at 900 °C for 8 hours in air.

Interconnects (10, 100)

Ferritic stainless steel, Crofer 22 APU or Crofer 22 H, 1.0 mm thickness, with integral air and fuel channels machined or embossed.

Operating conditions

Operating temperature 800 °C; cathode oxidant air with 3 volume percent H_2O; anode fuel humidified hydrogen (50:50 H_2:H_2O volumetric) as a reformate-equivalent test gas, with field service on natural-gas reformate compositions (H_2-CO-H_2O-CO_2) supported within the operating envelope; nominal current density 0.5 A/cm^2; nominal operating voltage 0.75 V per cell.

Expected accelerated-aging performance

ASR growth less than 2× the initial ASR over a 2000-hour accelerated-aging test at 800 °C with 3 volume percent cathode-side H_2O and a simulated Cr_2O_3 vapor source, compared against a baseline LSCF-GDC-YSZ cell of similar geometry whose ASR grows 3× to 5× under the same conditions. Projected curves are shown in Figure 6.

Accuracy note

The point values in this worked example derive from published SOFC-materials literature on spark-plasma-sintered GDC density versus processing parameters, LSCF A-site-deficit versus bulk conductivity, PrO_x infiltration versus cathode microstructure, and related topics. Specific values should be cross-checked against current literature and against the fabricator's own cell and materials data prior to reduction to practice. The filer asserts the compositional windows, process parameters, and dimensional ranges disclosed in §5 and §6 (rather than the point values in this §7) as the primary claim-equivalent scope of this disclosure.

§ 8

Enablement Statement

The specifications in §5 and §6 describe the integrated cathode-stack architecture in sufficient detail that a person of ordinary skill in the art (POSITA) of solid-oxide-fuel-cell materials and fabrication is able to reproduce the architecture without undue experimentation.

For purposes of this disclosure, a POSITA is a person possessing at least a master's-level or doctoral-level degree in materials science, ceramic engineering, chemical engineering, or a closely related field, with two or more years of direct experience in solid-oxide-fuel-cell cell or stack fabrication. The POSITA is familiar with standard SOFC processing equipment (tape-casting lines, lamination presses,

co-sinter furnaces rated to at least 1400 °C, spark-plasma-sintering apparatus, atomic-layer-deposition reactors, impedance-spectroscopy workstations, and scanning-electron-microscopy and X-ray-diffraction characterization tools) and with the published SOFC materials-science literature including the references cited in §3.

Commercial reagents for all disclosed compositions are available from standard suppliers at reagent grade or higher purity. Ba-rich perovskite powders in the (Ba,Sr)MnO_3 and (Ba,Sr)(Co,Fe)$O_{3-\delta}$ families are available as calcined single-phase powders from specialty ceramic suppliers including Fuel Cell Materials (Powell, OH), Kceracell (Pohang, South Korea), Praxair Specialty Ceramics, Sigma-Aldrich, and American Elements, and are synthesizable in-house from solid-state reaction or co-precipitation of the corresponding nitrate precursors. Praseodymium(III) nitrate hexahydrate, $Pr(NO_3)_3{\cdot}6H_2O$ at 99.9 percent purity, is available from Sigma-Aldrich, Alfa Aesar, and American Elements. GDC10 powder ($Ce_{0.9}Gd_{0.1}O_{1.95}$) with tap density appropriate for tape casting is available from Fuel Cell Materials, Kceracell, Sigma-Aldrich, and American Elements. The atomic-layer-deposition precursors $Ce(tmhd)_3$ and $Gd(tmhd)_3$ at sublimable grade are available from Strem Chemicals and Air Liquide Advanced Materials.

Process-validation methods appropriate for the disclosed architecture are standard in the field. These include scanning-electron-microscopy analysis of sublayer 40 grain-size distribution and porosity across the 40a-40b gradient; X-ray-diffraction phase identification of sublayer 40, cathode 50, and barrier 60 compositions; inductively-coupled-plasma mass-spectrometry for quantitative verification of post-infiltration PrO_x loading and cathode A-site stoichiometry; impedance spectroscopy at open-circuit voltage for area-specific-resistance measurement and for deconvolution of cathode and electrolyte contributions through the equivalent-circuit fits standard in the SOFC literature; and accelerated-aging chambers with controlled Cr vapor, humidity, and temperature as described in §5 and depicted in Figure 5.

No aspect of the integrated cathode-stack architecture requires non-standard equipment, non-commercial reagents, or processing conditions outside the range of conventional SOFC-fabrication practice. Reduction to practice is achievable by a POSITA using commercially available materials, instrumentation, and process tooling.

§ 9

Defensive Publication Clause

DEFENSIVE PUBLICATION UNDER 35 U.S.C. §102

The integrated cathode-stack architecture, and all compositional windows, process parameters, alternative embodiments, worked examples, and variants enumerated herein, including unrecited obvious variations a person of ordinary skill in the art would contemplate, are hereby disclosed as prior art under 35 U.S.C. §102 for defensive publication purposes effective 21 April 2026. This disclosure is intended to place the disclosed subject matter in the public domain and to preclude the issuance of valid patent claims on this subject matter filed after the publication date.

This disclosure is deposited as a preprint on Zenodo under DOI 10.5281/zenodo.19683758, with an additional preprint mirror on ChemRxiv pending moderation, and is archived as a dated PDF at the primary venue given in the filer block above. The filer retains archival copies of draft materials dated prior to the publication date for any subsequent inventorship or priority challenge. No patent applications have been filed by the filer on the disclosed subject matter, and the filer expressly disclaims any future patent filing on the disclosed architecture, components, compositional windows, process parameters, alternative embodiments, worked example, or covered variants.

§ 10

Figures

The figures below are referenced throughout §5 through §9. All figures use the reference-numeral key given in §5. Figures are schematic and illustrative; layer thicknesses in the cross-section figure are not drawn to scale.

§ 10.1 Figure 1. Repeat-unit cross-section

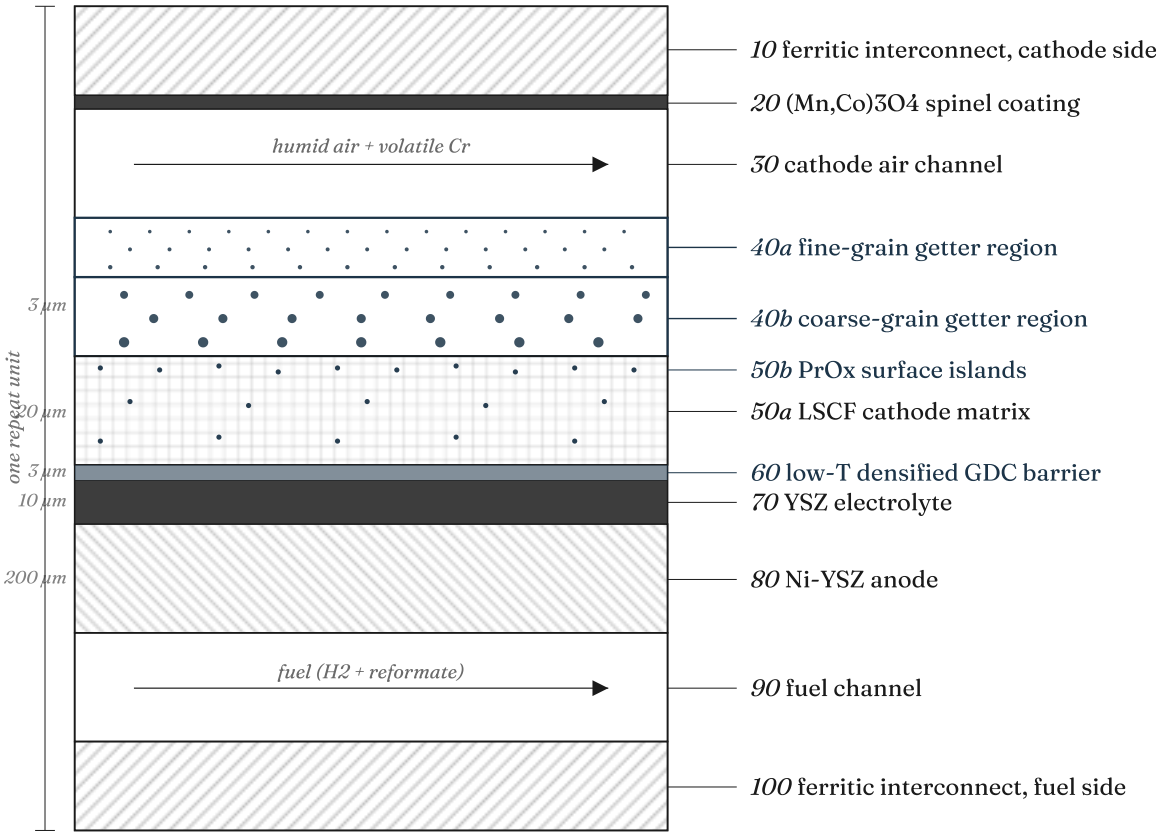

Figure 1. Cross-section of one SOFC repeat unit showing the three disclosed components (graded getter sublayer 40, PrO_x-infiltrated cathode 50, low-temperature-densified GDC barrier 60) and adjacent prior-art cell elements. Reference numerals follow the §5 key. The marine-shaded components are the disclosed subject matter. Layer thicknesses shown are schematic and not to scale.

§ 10.2 Figure 2. Grain-size grading profile through sublayer (40)

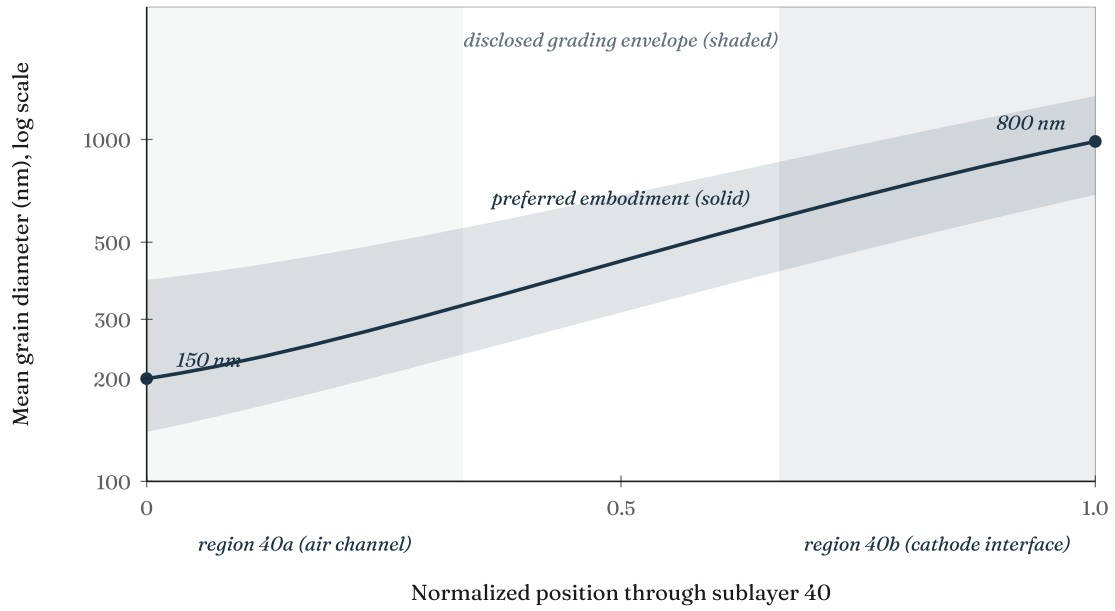

Figure 2. Mean grain diameter as a function of normalized position through getter sublayer 40, from the air-channel-facing side (region 40a, position 0) to the cathode-interface-facing side (region 40b, position 1). The preferred embodiment (solid curve) grades continuously from 150 nm at position 0 to 800 nm at position 1. The shaded envelope shows the full disclosed grading window: 100 to 300 nm at position 0, widening to 500 to 1000 nm at position 1.

§ 10.3 Figure 3. Thermodynamic stability ladder, alkaline-earth chromates

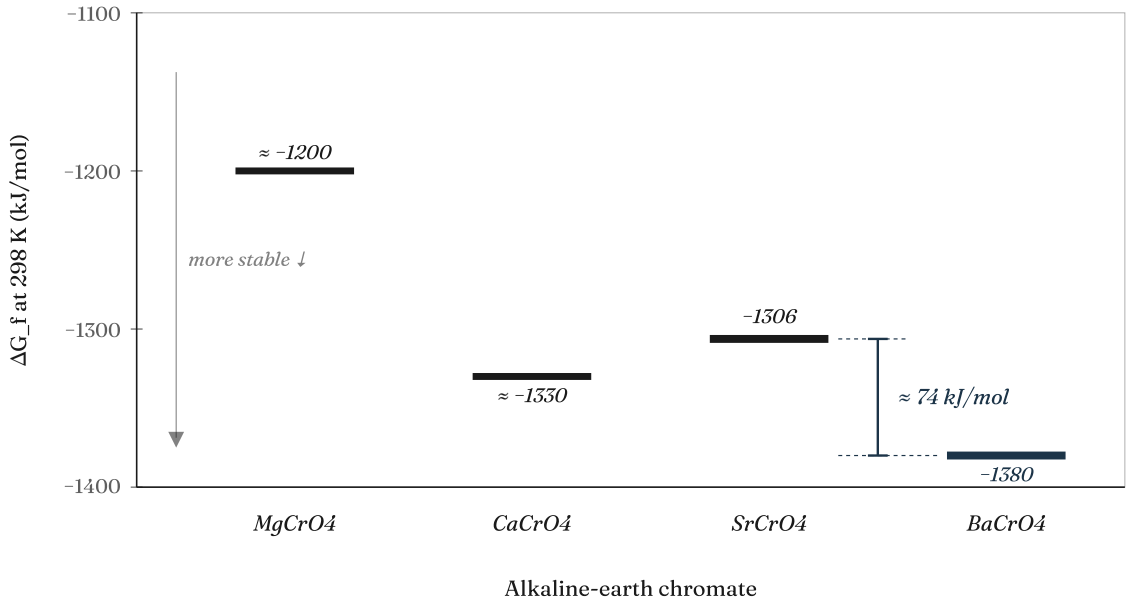

Figure 3. Standard Gibbs free energy of formation for the alkaline-earth chromate phases, plotted from least stable ($MgCrO_4$, top) to most stable ($BaCrO_4$, bottom). The gap of approximately 60 to 80 kJ/mol between $SrCrO_4$ and $BaCrO_4$ drives thermodynamic redirection of volatile-Cr capture from the LSCF cathode 50 to the Ba-rich sublayer 40. Anchor values shown are representative; exact ΔG_f values vary across published thermochemical compilations (see §3 prior-art entry on thermochemical compilations). Values for $CaCrO_4$ and $MgCrO_4$ are approximate and are included for periodic-trend context.

§ 10.4 Figure 4. Cell co-sinter schedule

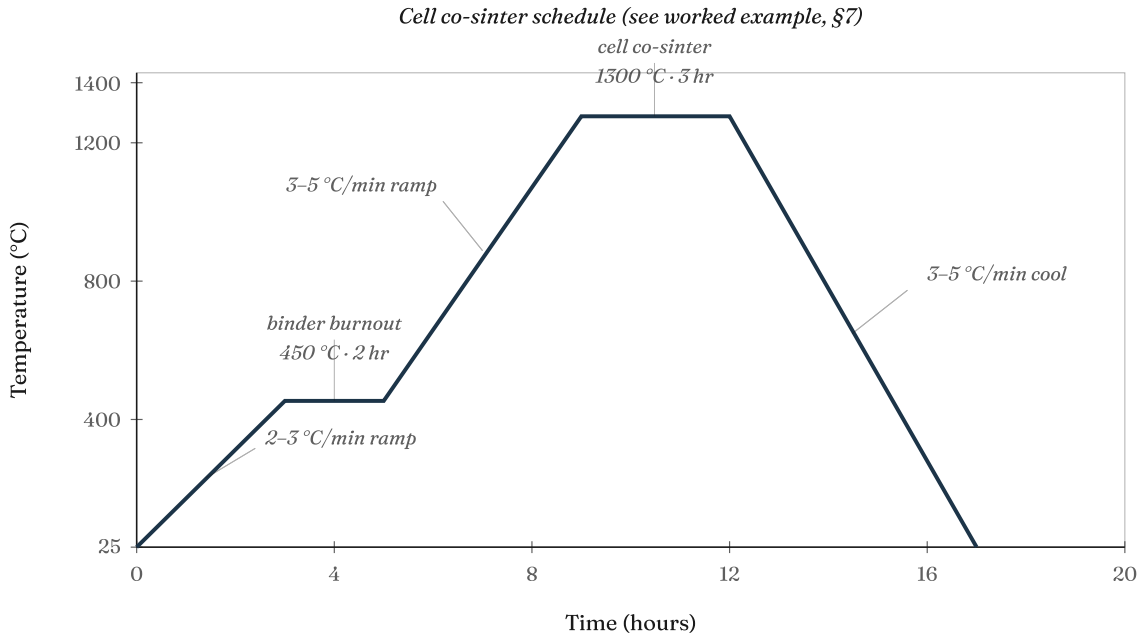

Figure 4. Temperature-vs-time profile for the cell co-sinter schedule of §5.4 and the worked example of §7. Binder burnout at 450 °C for 2 hours after a 2 to 3 °C/min ramp. Primary co-sinter at 1300 °C for 3 hours after a 3 to 5 °C/min ramp. Cool at 3 to 5 °C/min. Post-sinter wet infiltration and PrO_x decomposition at 550 °C for 1.5 hours is a separate thermal event on a subsequent run and is not included on this chart.

§ 10.5 Figure 5. Accelerated-aging test setup schematic

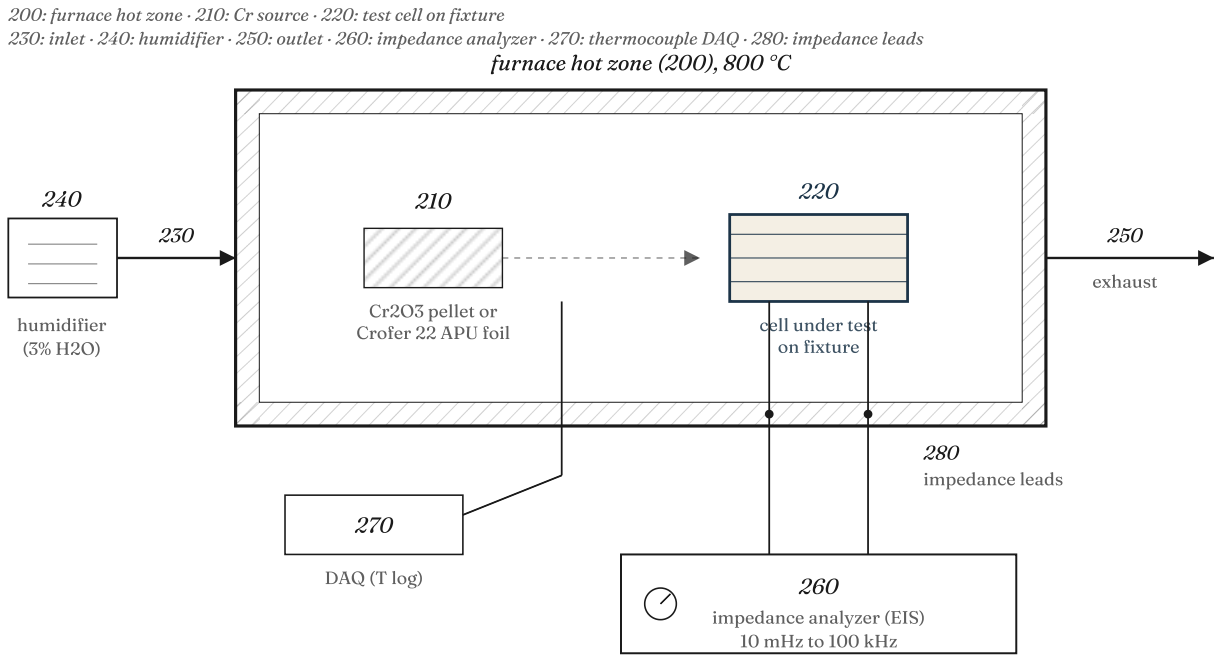

Figure 5. Schematic of the accelerated-aging test rig referenced in §5 and in the worked example of §7. Humidified air (3 volume percent H_2O) enters through gas inlet 230 after passing humidifier 240, flows across chromium source 210 (Crofer 22 APU foil coupon or Cr_2O_3 pellet) inside furnace hot zone 200 at 800 °C, reaches cell under test 220 on the test fixture, and exits through gas outlet 250. Cell impedance is measured through leads 280 by impedance analyzer 260 at 250-hour intervals over a 2000-hour total test duration. Thermocouple 270 logs hot-zone temperature to the data-acquisition system. Reference numerals in the 200-series are used for test-rig elements and do not reference cell elements.

§ 10.6 Figure 6. Projected ASR growth, baseline and intervention

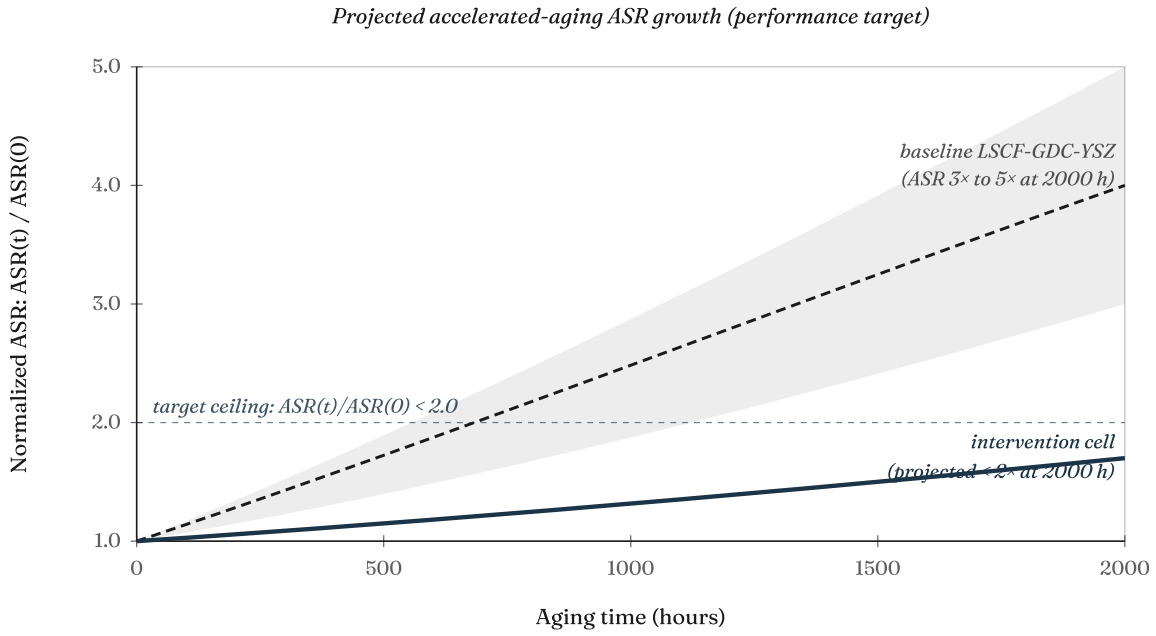

Figure 6. Projected normalized area-specific-resistance growth over 2000 hours of accelerated aging at 800 °C with 3 volume percent H_2O in cathode air and a Cr_2O_3 vapor source. The baseline LSCF-GDC-YSZ cell (dashed center trace with shaded 3× to 5× envelope) represents typical published performance for cells without the three disclosed interventions. The intervention cell (solid marine curve) represents the performance target of below 2× ASR growth for cells incorporating all three disclosed components per §5. Curves represent a performance target; reduction-to-practice measurement is required to establish the actual magnitudes.

End of Technical Disclosure 01. See Research Note 01 for the narrative-register companion. For commissioned implementation work see Engagements.